

# COMPTEL detection of low-energy gamma rays from the HVC Complex M and A region?

J.J. Blom<sup>2</sup>, H. Bloemen<sup>2,5</sup>, A.M. Bykov<sup>4,2</sup>, W.B. Burton<sup>5</sup>, Dap Hartmann<sup>6</sup>, W. Hermsen<sup>2</sup>, A.F. Iyudin<sup>1</sup>, J. Ryan<sup>3</sup>, V. Schönfelder<sup>1</sup>, A.W. Strong<sup>1</sup>, and Yu.A. Uvarov<sup>4</sup>

<sup>1</sup> Max-Planck-Institut für extraterrestrische Physik, P.O. Box 1603, D-85740 Garching, Germany

<sup>2</sup> SRON-Utrecht, Sorbonnelaan 2, 3584 CA Utrecht, The Netherlands

<sup>3</sup> Space Science Center, Univ. of New Hampshire, Durham NH 03824, USA

<sup>4</sup> A.F. Ioffe Institute of Physics and Technology, 194021 St. Petersburg, Russia

<sup>5</sup> Leiden Observatory, P.O. Box 9513, 2300 RA Leiden, The Netherlands

<sup>6</sup> Center for Astrophysics, 60 Garden St., MS 72, Cambridge, MA 02138, USA

Received 22 August 1996 / Accepted 7 October 1996

**Abstract.** We report the first observational indication for extended MeV emission that may be associated with high-velocity clouds (HVCs). Based on a combination of fifteen COMPTEL observations made during the period 1991–1995 we find evidence for intense  $\gamma$ -radiation at 0.75–3 MeV from the general direction of the HVC Complexes M and A, adjacent to the Lockman et al. hole. The  $\gamma$ -ray excess roughly covers a region of exceptionally low H I column densities and appears to consist of a time-variable source and persistent, likely diffuse, emission. The (enhanced) diffuse soft X-rays from this HVC area seen by ROSAT may be closely related to the  $\gamma$ -ray emission. We show that the X-ray and  $\gamma$ -ray emission can both be attributed to non-thermal electron bremsstrahlung arising from HVC interactions with the galactic disk or lower halo.

**Key words:** gamma rays: observations – ISM: clouds – ISM: individual objects: HVC Complex M, Complex A

## 1. Introduction

We discuss the COMPTEL detection of (extended) MeV  $\gamma$ -radiation from a sky region bounded by  $30^\circ < b < 70^\circ$ ,  $200^\circ > l > 140^\circ$ . Preliminary large-scale COMPTEL maps at MeV energies (Schönfelder et al. 1996) already showed evidence for emission from this area; a pronounced time-variable source component is discussed by Iyudin et al. (1996). This area contains several interesting features that are known from H I 21-cm studies — the Lockman et al. hole (1986) centered at  $(l, b) \approx (150^\circ, 55^\circ)$  and the main parts of the HVC Complexes M and A. These structures are clearly seen in the Leiden/Dwingeloo 21-cm survey (Hartmann 1994; Hartmann & Burton 1996) as well.

*Send offprint requests to:* J.J. Blom (H.Blom@sron.ruu.nl)

A comparison between results of this survey and a combination of fifteen COMPTEL observations shows an intriguing (anti-) correlation, suggesting that HVC interactions with the galactic disk or lower halo may cause emission of non-thermal high-energy photons.

Some evidence for interactions of high-velocity clouds (HVCs) with the galactic disk or lower halo has been found from H I 21-cm observations in the anti-centre region (e.g. Burton & Moore 1979; Mirabel 1982; Mirabel & Morras 1990) and in the direction of the Draco Nebula (Kalberla et al. 1984). Evidence for soft X-ray emission associated with HVCs is seen in the Draco region based on observations by SAS-3, HEAO-1, and the Wisconsin rocket missions (Hirth et al. 1985) and by ROSAT (Kerp et al. 1994). Recently, Herbstmeier et al. (1995) found diffuse  $\frac{1}{4}$  keV emission from the HVC Complex M region in the ROSAT observations. They detected X-ray edge-brightening around the cloud cores, which might also arise from HVC interactions with ambient matter. Morfill & Tenorio-Tagle (1983) discussed the development of strong shocks during such energetic interactions and the subsequent acceleration of charged particles and  $\gamma$ -ray production in the 100 MeV regime. So far, no compelling evidence for  $\gamma$ -ray emission from the HVCs has been found, although the excess  $\gamma$ -ray emission in the galactic plane near  $l \approx 18^\circ$  may be related to Complex C (Bloemen 1989).

## 2. Instrument and analysis methods

COMPTEL is sensitive to photons in the 0.75 to 30 MeV range with an energy resolution of 5–10% FWHM. Within its wide field of view of about 1 steradian the instrument is able to locate  $\gamma$ -ray sources with an accuracy of typically  $1^\circ$ . A detailed description of COMPTEL and its detection principle is given by Schönfelder et al. (1993).

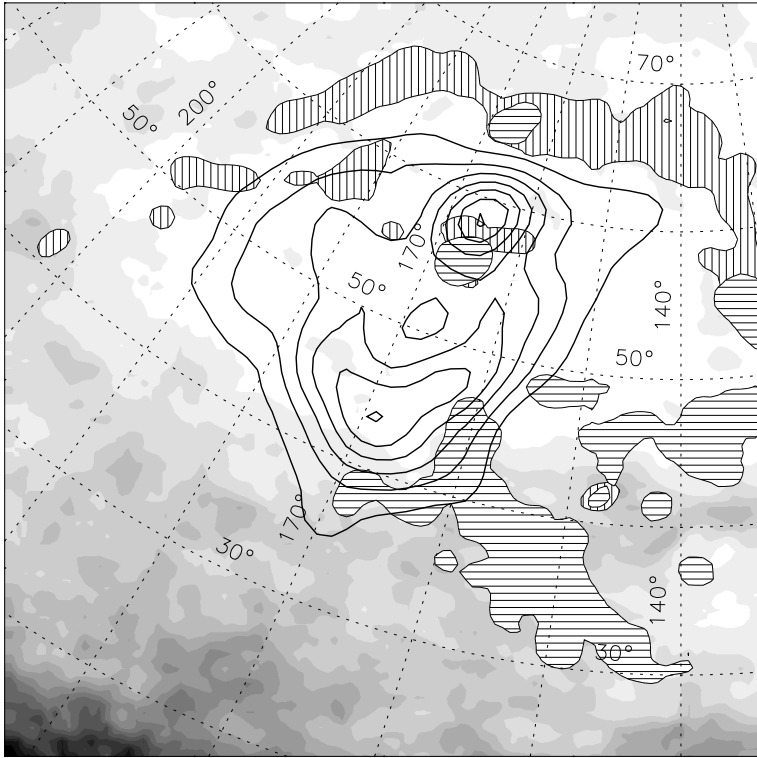


**Fig. 1.** Superposition of the  $\gamma$ -ray likelihood map from the combined COMPTEL observations (0.75–3 MeV) and the HI distribution of the HVC Complex M and A region from the Leiden/Dwingeloo survey. **Gamma-rays:** *solid contours:* at  $-2 \ln \lambda = 11$  step 10. **HI column density:** *Grey scales:* integrated over  $V_{\text{lsr}} > -70 \text{ km s}^{-1}$  (white corresponds to densities  $< 2 \times 10^{20} \text{ cm}^{-2}$  and black to densities  $> 1 \times 10^{21} \text{ cm}^{-2}$ ). *Vertically hatched contours:* high-velocity components in the range  $-120 \text{ km s}^{-1} < V_{\text{lsr}} < -70 \text{ km s}^{-1}$  (column density  $> 1.5 \times 10^{19} \text{ cm}^{-2}$ ). *Horizontally hatched contours:* high-velocity components with  $V_{\text{lsr}} < -120 \text{ km s}^{-1}$  (column density  $> 1 \times 10^{19} \text{ cm}^{-2}$ ). An  $(l, b)$  grid is superimposed. The corners of the map are not fully covered by the limited set of COMPTEL observations used here.

The telescope events are binned in a 3-dimensional (3D) data space. Imaging involves the identification of 3D structures in this data space that are characteristic for sources. Sky maps are obtained by applying either a maximum-likelihood method (de Boer et al. 1992) or a maximum-entropy deconvolution (Strong et al. 1992). The first technique directly provides flux estimates and statistical significances of sources identified in the data. The maximum-entropy analysis yields photon intensity images. In this work, the required background model for both methods was generated by applying a running-average filter technique to the 3D data space. The basic features are described by Bloemen et al. (1994).

### 3. Observations and analysis

The CGRO observation programme consists of four phases (e.g. Gehrels et al. 1994). Observations covering the sky area between Complex M and A from all phases are used in this work, i.e. CGRO viewing periods of Phase I (4, 18, 40), Phase II (216, 218, 222, 227, 228), Phase III (319, 319.5, 322, 326), and Phase IV (411.1, 411.5, 418).

We made maximum-likelihood ratio maps in the four standard energy intervals (0.75–1 MeV, 1–3 MeV, 3–10 MeV, and 10–30 MeV) for all individual observations. No significant source signature was seen in the maps above 3 MeV from the general direction of the HVC complexes. By contrast, below 3 MeV we find indications for  $\gamma$ -ray emission in nearly every observation. The features are partly extended and spatially not fully consistent with each other. This may indicate that variable sources are present, but could as well be due to known limita-

tions of our technique for mapping extended emission in case of limited statistics, as seen in simulations discussed below.

In order to improve the statistics, we combined all observations and repeated the likelihood analysis in the standard energy intervals. Again, the maps for the 0.75–1 MeV and 1–3 MeV ranges show distinct emission with high significance (addressed below), whereas no emission is seen above 3 MeV. Figure 1 shows the maximum-likelihood map for the combined observations in the 0.75–3 MeV range.

Two local maxima in likelihood are seen in Fig. 1: one prominent feature centered at  $(l, b) \approx (169^\circ, 43^\circ)$  and a second one at  $(l, b) \approx (165^\circ, 57^\circ)$ . The first maximum is near the EGRET sources 2EG J0917+4420 and 2EG J0957+5515 (Thompson et al. 1995). No other EGRET sources are seen in the extended emission region we observed. The second COMPTEL peak, designated GRO J1040+48, is discussed by Iyudin et al. (1996) based on Phase I and Phase II observations. They argue that GRO J1040+48 might be time-variable. Indeed, we find some evidence for flux variability of this particular component as well. For instance, we find a  $3\sigma$  decrease in flux (0.75–3 MeV) of the Iyudin et al. source from  $(2.4 \pm 0.3) \times 10^{-4}$  for the sum of Phase I/II viewing periods to  $(0.7 \pm 0.4) \times 10^{-4} \text{ ph cm}^{-2} \text{ s}^{-1}$  for Phase III/IV. This flux is only  $\lesssim 15\%$  of the total emission seen, which suggests that either a combination of extended emission (see next section) with possibly one or two point sources is visible in the map, or more than two point sources are required to explain the observed  $\gamma$ -radiation.

Because of its extended appearance (with no a priori model prediction available), the significance of the observed emission is difficult to quantify. In general, we use the quantity  $-2 \ln \lambda$

to define statistical significances, where  $\lambda$  is the maximum-likelihood ratio, i.e. the ratio between the maximum likelihood of a fit with a background model only and that of a fit with a sky model included (which may be just a single source or a more complex ensemble). In order to give some indication of the detection significance at this stage (we return to this point in the next section), we note that the peak  $-2 \ln \lambda$  values in our maps are 30.9 at  $(l, b) \approx (165^\circ, 57^\circ)$  and 46.5 at  $(l, b) \approx (163^\circ, 47^\circ)$  in the 0.75–1 and 1–3 MeV ranges, respectively. These values are equivalent to  $4.9\sigma$  and  $6.2\sigma$  detections (interpreting  $-2 \ln \lambda$  in terms of a  $\chi^2$  distribution with 3 degrees of freedom). For comparison, we have learned from simulations that the chance probability of finding a statistical fluctuation with  $-2 \ln \lambda = 30.9$  in an all-sky search for sources in four energy intervals is  $\sim 2 \times 10^{-3}$ ; for  $-2 \ln \lambda = 46.5$  this probability is  $\sim 10^{-6}$ . Clearly, the likelihood values of the peaks in Fig. 1 at 0.75–3 MeV correspond to even higher detection significances ( $-2 \ln \lambda > 60$  for both peaks).

The HI column density gray scales from the Leiden/Dwingeloo 21-cm survey in Fig. 1 indicate a remarkable anti-correlation with the MeV emission — the  $\gamma$ -ray excess appears to cover an extended region of very low column density which is bounded by HVC Complex M ridges at  $b \approx 65^\circ$  and an arc shaped feature at the high-latitude end of the Complex A ridge ( $b \approx 40^\circ - 45^\circ$ ). This suggests a physical connection between the HI distribution and the  $\gamma$ -ray emission in this region.

The enhanced soft X-ray emission that was detected by ROSAT (Herbstmeier et al. 1995) in the sky area  $50^\circ < b < 65^\circ$ ,  $190^\circ > l > 160^\circ$  partly correlates with the  $\gamma$ -ray excess at high latitudes near Complex M. This provides an interesting additional hint for interactions between HVCs and matter from the galactic disk or lower halo. It is not yet clear if the  $\gamma$ -rays seen below  $b \sim 50^\circ$  in the vicinity of Complex A are associated with enhanced X-radiation, because the presence in the ROSAT data of diffuse X-rays from this region has not been studied so far.

#### 4. Simulations

For the  $\gamma$ -ray excesses at  $(l, b) \approx (169^\circ, 43^\circ)$  and  $(l, b) \approx (165^\circ, 57^\circ)$  we find fluxes of respectively  $(2.0 \pm 0.2) \times 10^{-4}$  and  $(1.9 \pm 0.2) \times 10^{-4}$  ph cm $^{-2}$  s $^{-1}$  at 0.75–3 MeV for the combination of all observations. We performed simulations and model fitting to estimate the total flux of the observed  $\gamma$ -ray emission, and conclude that this total flux is about 4 times higher than the summed flux of the two excesses, namely  $(1.5 \pm 0.1) \times 10^{-3}$  ph cm $^{-2}$  s $^{-1}$ . Only statistical uncertainties are given here.

We applied our imaging tools to simulated COMPTEL observations (0.75–1 and 1–3 MeV) that include a simple extended source. These simulations contain the same instrumental and background characteristics as the combination of the real observations discussed above. The adopted source model has a 2-dimensional Gaussian shape with a FWHM of  $20^\circ$ . This size is comparable to the typical dimension of the observed  $\gamma$ -ray excess. The maximum-likelihood maps of these simulations look very similar to the real observations if we use input fluxes of typically  $(5 - 7) \times 10^{-4}$  ph cm $^{-2}$  s $^{-1}$  in each band. Likeli-

hood fitting of this simple model to the real observations leads to comparable flux estimates and  $-2 \ln \lambda$  values as high as 84 and 234 for 0.75–1 and 1–3 MeV, respectively. As an alternative approach to estimate total fluxes, we simultaneously fitted several point sources spread over the observed emission region and obtained very similar results.

#### 5. Non-thermal electrons in HVCs

If the observed emission is indeed largely of diffuse nature, the  $\gamma$ -ray emissivity has to be significantly enhanced in this region of the sky. The  $\gamma$ -ray intensity expected from a typical emissivity as determined for the galactic disk, namely  $\sim 5 \times 10^{-25}$  photon Hatom $^{-1}$  s $^{-1}$  ster $^{-1}$  MeV $^{-1}$  at 1 MeV (Strong et al. 1994), is 2–3 orders of magnitude lower than observed. The interaction of HVCs with the matter and electromagnetic fields of the galactic disk or lower halo seems a natural source of non-thermal emission. If the total mass of the clouds involved is of the order  $10^4 M_\odot$ , a typical speed of 100 km s $^{-1}$  then implies a kinetic energy of  $10^{51}$  erg. A precise calculation of the expected X-ray and  $\gamma$ -ray emission is not feasible, because information on the magnetic field structure is lacking and most physical parameters involved are uncertain by at least a factor of two. We describe here a quantitative model that attributes the observed X-ray and  $\gamma$ -ray emission to bremsstrahlung from locally accelerated electrons interacting with the HVC gas using plausible parameter values.

Adopting for the lower galactic halo a temperature  $T \sim (2 - 4) \times 10^5$  K, a number density  $n \sim 3 \times 10^{-3}$  cm $^{-3}$ , and a magnetic field strength  $B \sim 1 \mu\text{G}$  (see e.g. Bloemen 1987), it follows that the adiabatic sound velocity is  $\sim 55 - 75$  km s $^{-1}$  and the local Alfvén velocity  $\sim 35$  km s $^{-1}$ . In such an environment, HVCs with velocities of  $\sim 100 - 200$  km s $^{-1}$  can be expected to produce strong local disturbances and bow shocks with moderate magnetosonic Mach numbers  $M$  of 1.7–3 for both quasi-parallel and quasi-perpendicular waves. This is sufficient to consider the shock waves to be supercritical (Kennel et al. 1985).

The basic characteristics of supercritical collisionless shock waves are fairly well understood from numerical simulations by hybrid codes, which treat the protons as particles and the electrons as a fluid (e.g. Jones & Ellison 1991). The spectra of accelerated electrons cannot be obtained from a pure hybrid code, but Bykov & Uvarov (1995) proposed a method to calculate the electron distribution function in the vicinity of a quasi-parallel shock with moderate Mach number. It was shown that the vortical fluctuations of electric fields induced by random fluxes of ions in the supercritical shock transition region are responsible for a stochastic pre-acceleration and heating on scales of the order of the collisionless shock width.

We applied the code developed by Bykov & Uvarov (1995) with the parameters as given above and traced the shock-accelerated electrons when they penetrate into the HVC gas ( $N_H \sim 10^{20}$  cm $^{-2}$ ), taking into account Coulomb losses and diffusion transport with a momentum-dependent mean free path  $\Lambda(p) \propto p^{0.5}$ . The bremsstrahlung emissivities were calculated

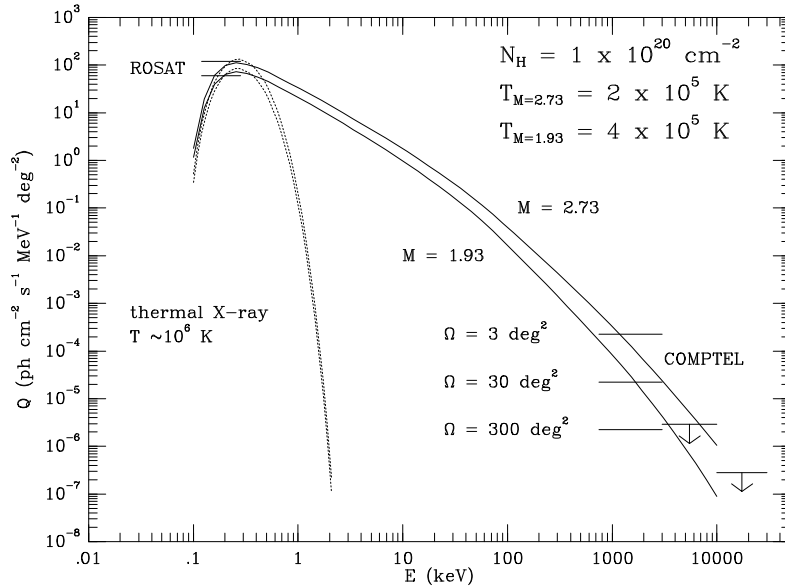


**Fig. 2.** Model HVC bremsstrahlung spectra for two typical HVC-shock magnetosonic Mach numbers compared with Complex M intensity measurements by ROSAT and COMPTEL. The maximum variation in the observed ROSAT X-ray intensities is shown by two horizontal lines (from Herbstmeier et al. 1995). The COMPTEL intensity depends on the total solid angle  $\Omega$  of the  $\gamma$ -ray emission area (only the total flux is measured); three intensity levels are shown (see text). Adopted values for the plasma temperatures at HVC shock upstream and for the intervening HI column density are indicated. *Dotted lines*: Modelled thermal X-ray spectra.

as a function of penetration depth into the cloud (omitting the effect of possible heavy elements inside the cloud) and then the integrated photon intensity spectrum was derived. The column density of the gas ( $N_H$ ) involved in the  $\gamma$ -ray production may be uncertain, but we have verified that this does not drastically affect our findings here. Photoelectric absorption by intervening matter ( $\sim 10^{20} \text{ cm}^{-2}$ ) that affects the soft X-ray part of the spectrum was taken into account using the cross sections and abundances given by Morrison & McCammon (1983).

Figure 2 shows the predicted spectra for typical physical parameters as given above, together with the soft X-ray intensities measured by ROSAT (Herbstmeier et al. 1995) and the 0.75–3 MeV  $\gamma$ -ray intensities measured by COMPTEL. The two ROSAT intensity levels reflect the maximum variation in the observed soft X-ray foreground counts:  $\sim (500 - 1000) \times 10^{-6} \text{ cts s}^{-1} \text{ arcmin}^{-2}$ . The COMPTEL intensity depends on the actual size of the emission region(s), which we cannot derive from the  $\gamma$ -ray images. As a lower limit, we can take the solid angle covered by the M IV cloud (a few  $\text{deg}^2$ ). A solid angle of  $300 \text{ deg}^2$  is taken as the maximum  $\gamma$ -ray emission area, i.e. the size of a 2-dimensional Gaussian with FWHM of 20 deg that was used for model fitting an extended source. In Fig. 2, we show the intensity levels for 3, 30 and  $300 \text{ deg}^2$ , adopting an integrated flux (0.75–3 MeV) of  $1.5 \times 10^{-3} \text{ ph cm}^{-2} \text{ s}^{-1}$  as obtained in Sect. 4. Upper limits for energies above 3 MeV for  $3 \text{ deg}^2$  are indicated as well. For comparison, thermal X-ray spectra for a temperature of  $\sim 10^6 \text{ K}$  are shown. We conclude that the model estimates are in good agreement with the ROSAT and COMPTEL measurements.

Clearly, the parameter values used for our model calculations may not apply. We emphasize that our main purpose here is to show that HVC interactions with the ambient medium can *in principle* account for the observed  $\gamma$ -ray emission.

As shown above, the shock acceleration model predicts X-ray and  $\gamma$ -ray intensity levels that are in agreement with the

ROSAT and COMPTEL detections, but a detailed *spatial* correspondence between the soft X-ray and  $\gamma$ -ray emission is not observed. We emphasize that this is indeed expected in the scenario discussed here. In contrast to the thermal electrons (emitting the X-rays), the high energy electrons are able to penetrate deeply into the intervening matter and subsequently escape from the boundary of the clouds. The  $\gamma$ -ray emission region can therefore be much larger than the diffuse X-ray emission region.

In an alternative scenario, Kerp et al. (1994) propose that magnetic reconnection may be the main process responsible for plasma heating and particle acceleration. A comparison between quantitative predictions of this mechanism and the shock acceleration estimates described above would be of great interest.

## 6. Conclusions

We conclude that the  $\gamma$ -radiation observed by COMPTEL from the sky region between the HVC Complexes M and A may be largely due to non-thermal emission arising from HVC interactions with the galactic disk or lower halo. Supporting arguments are:

- The  $\gamma$ -ray emission seen from the general direction of the HVC complexes cannot be attributed to a single source and is probably (mostly) of diffuse nature. This interpretation is supported by simulations and model fitting.
- The positional anti-correlation of the HVC complexes and the  $\gamma$ -ray excess is striking. The  $\gamma$ -ray peak at  $(l, b) \approx (165^\circ, 57^\circ)$  is consistent with the fastest moving M IV cloud, though its variable nature seems to rule out HVC-related emission (alternative identifications have been discussed by Iyudin et al. 1996).
- Enhanced X-ray emission is seen by ROSAT in the same sky area (Herbstmeier et al. 1995). The shock-acceleration model of Bykov & Uvarov (1995) can account for non-

thermal X-ray and  $\gamma$ -ray intensities in agreement with the ROSAT and COMPTEL detections.

Studies of other HVC  $\gamma$ -ray emission regions are in progress.

*Acknowledgements.* The COMPTEL project is supported by the German government through DARA grant 50 QV 90968, by NASA under contract NAS5-26645, and by the Netherlands Organisation for Scientific Research (NWO). A.M.B and Yu.A.U acknowledge partial financial support by RBRF grant 95-02-4143a. We thank Lucien Kuiper for his help in composing the grey scale image and our colleagues from the Astrophysics Division of ESA for their contribution to and continuing support of COMPTEL.

## References

- Bloemen H., 1987, ApJ 322, 694  
Bloemen H., 1989, in "Structure and dynamics of the ISM" eds. G. Tenorio-Tagle et al., Springer-Verlag, p.494  
Bloemen H., Hermsen W., Swanenburg B.N., et al., 1994, ApJS 92, 419  
Burton W.B., Moore R.L., 1979, AJ 84, 189  
Bykov A.M., Uvarov Yu.A., 1995, in "Proc. 24th Int. Cosmic Ray Conf.", Rome, 3, p.241  
de Boer H., Bennett K., Bloemen H., et al., 1992, in "Data Analysis in Astronomy IV" eds. V. Di Gesù et al., Plenum, New York, 59, 241  
Gehrels N., Chipman E., Kniffen, D.A., 1994, in "Proc. Second Compton Symposium", eds. C.E. Fichtel et al., AIP Conf. Proc. 304, 3  
Hartmann D., 1994, Ph.D. thesis, University of Leiden  
Hartmann D., Burton W.B., 1996, "Atlas of Galactic Neutral Hydrogen", Cambridge University Press, in press  
Herbstmeier U., Mebold U., Snowden S.L., et al., 1995, A&A 298, 606  
Hirth W., Mebold U., Müller P., 1985, A&A 153, 249  
Iyudin A., Bennett K., Bloemen H., et al., 1996, A&A 311, L21  
Jones F.C., Ellison D.C., 1991, Space Sci. Rev. 58, 259  
Kalberla P.W.M., et al., 1984, in "Local Interstellar Medium", eds. Y. Kondo et al., IAU Coll. 81, 243  
Kennel C.F., Edmiston J.P., Hada T., 1985, in "Collisionless Shocks in the Heliosphere" eds. B. Tsurutani et al., Washington, AGU, 1  
Kerp J., Lesch H., Mack K.-H., 1994, A&A 286, L13  
Lockman F.J., Jahoda K., McCammon D., 1986, ApJ 302, 432  
Mirabel I.F., 1982, ApJ 256, 112  
Mirabel I.F., Morras R., 1990, ApJ 356, 130  
Morfill G., Tenorio-Tagle G., 1983, Space Sci. Rev. 36, 93  
Morrison R., McCammon D., 1983, ApJ 270, 119  
Schönfelder V., Aarts H., Bennett K., et al. 1993, ApJS 86, 657  
Schönfelder V., et al., 1996, A&A submitted  
Strong A.W., Cabeza-Orcel P., Bennett K., et al., 1992, in "Data Analysis in Astr. IV" eds. V. Di Gesù et al., Plenum, New York, 59, 251  
Strong A.W., Bennett K., Bloemen H., et al., 1994, A&A 292, 82  
Thompson D.J., Bertsch D.L., Dingus B.L., et al., 1995, ApJS 101, 259